Small-Angle X-ray Scattering and Dielectric Relaxation Studies of the Order−Disorder Transition of Semidilute Solutions of Polystyrene-*block*-Polyisoprene

Naoki Sakamoto and Takeji Hashimoto*

Department of Polymer Chemistry, Graduate School of Engineering, Kyoto University, Kyoto 606-01, Japan

Ryota Kido and Keiichiro Adachi*

Department of Macromolecular Science, Graduate School of Science, Osaka University, Toyonaka, Osaka 560, Japan

Received July 1, 1996; Revised Manuscript Received September 16, 1996[⊗]

ABSTRACT: The order−disorder transition (ODT) of semidilute solutions of polystyrene-*block*-polyisoprene in toluene was studied by small-angle X-ray scattering (SAXS) and dielectric relaxation. Both methods clearly revealed, for the first time for a semidilute solution, a sharp order−disorder transition at the same order−disorder transition temperature. The SAXS studies indicated that the ODT is the thermally induced first-order phase transition from the "non-mean-field disordered state" to an ordered state.

I. Introduction

The order−disorder transition (ODT) of block copolymer melts has been extensively studied both theoretically and experimentally.[1−6] The experimental studies for the melts have been pursued for block copolymers with relatively small segregation power χN by means of small-angle X-ray scattering (SAXS),[6−10] small-angle neutron scattering,[5] low-frequency rheology,[5,11] birefringence,[12−14] depolarized light scattering[15] and dielectric relaxation spectroscopy.[16] Here χ is the segmental interaction parameter, and N is total degree of polymerization of the block copolymers. All the properties obtained from the above methods showed a sharp discontinuous change at ODT, which has been interpreted as the thermally induced first-order phase transition.[4]

However, the nature of ODT for semidilute or concentrated block copolymer solutions has been left relatively unexplored. Therefore, in this work we focus on this particular problem and investigate semidilute solutions of polystyrene-*block*-polyisoprene (SI) with SAXS and dielectric relaxation. Recently, the effect of ODT on dynamics in semidilute and concentrated solutions of SI was studied by several authors using dynamic light scattering[17−20] and birefringence.[21] Yao et al.[22] reported the dielectric normal mode relaxation[23] of the polyisoprene (PI) block chains in concentrated solutions of a symmetrical SI in toluene which exhibited bimodal dielectric loss curve below a critical temperature. They believed that the critical temperature was the T_{ODT} of the SI solution but did not make the morphology analyses in terms of scattering experiments such as SAXS. We shall report here that the semidilute solution also exhibits a sharp ODT due to the thermally induced first-order phase transition studied using SAXS and dielectric methods.

II. Experimental Methods

II-A. Sample. A SI diblock copolymer coded as SI(92−80) was synthesized by living anionic polymerization. First, living polyisoprene was prepared at 290 K in *n*-heptane with *sec*-butyllithium as the initiator. The monomer concentration was ca. 3 wt %. Subsequently two-thirds of the heptane was replaced by benzene through vacuum distillation. Then styrene was allowed to polymerize at room temperature for 48 h. The polymerization reaction was terminated with methanol.

The weight- and number-average molecular weights (M_w and M_n) were measured by a gel permeation chromatograph (GPC; Tosoh Model HLC-801A) equipped with a detector of low-angle light scattering (Tosoh; LS-8000). The styrene content was determined from the absorbance at 257 nm. The M_w of the SI, polystyrene (PS), and PI block chains are 172, 92, and 80×10^3, respectively. The polydispersity index (M_w/M_n) of the SI is 1.08.

In this study, toluene solutions of SI(92−80) were used as the sample. The SAXS sample was prepared by dissolving SI(92−80) in an excess amount of toluene and evaporating toluene slowly until the polymer concentration became 20, 25, and 30 wt %. Then, the given solution was rapidly transferred into the sample cell for the SAXS measurements. For dielectric measurements, prescribed amounts of SI(92−80) and toluene (Wako 99.8% pure) were sealed in a bottle together with a magnetic stirrer chip coated with Teflon and stirred until the solution became homogeneous (ca. 2 days). The concentration was remeasured before the solution was transferred into the dielectric cell.

II-B. SAXS. SAXS was measured *in situ* at each temperature with a SAXS apparatus which consists of an 18-kW rotating-anode X-ray generator (MAC Science Co. Ltd., Japan), a graphite crystal for incident-beam monochromatization, a 1.5-m camera (0.5 m from the source to the sample and 1.0 m from the sample to the detector), and a one-dimensional position-sensitive proportional counter (PSPC). The basic part of the apparatus is the same as that reported previously,[24] except for a new X-ray generator. The Cu Kα line ($\lambda = 0.154$ nm) was used. The sample temperature was controlled with an accuracy of ±0.03 °C with a temperature enclosure and controller constructed in our laboratory. The sample cell used in this measurement is basically similar to the one which was described elsewhere.[25] Both sides of the window were sealed by Kapton films of 14 μm thickness. These films were adhered to the cell to prevent toluene evaporating from the gap between the films and the sample cell. We confirmed that the concentration of the solution did not change in this experiment by checking the weight of the sample before and after measurement. The SAXS measurement was performed in a slow cooling cycle from 318 K. At each measuring temperature the

[⊗] Abstract published in *Advance ACS Abstracts,* November 1, 1996.

S0024-9297(96)00948-5 CCC: $12.00 © 1996 American Chemical Society

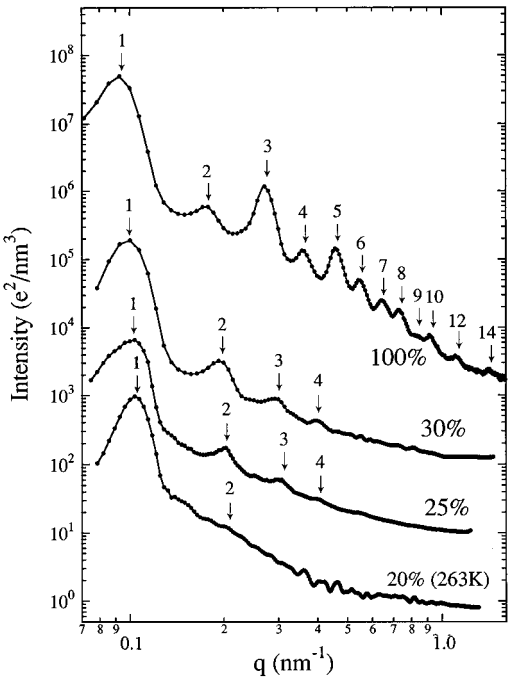

Figure 1. SAXS profiles plotted in double logarithmic scale at various polymer concentrations and at room temperature (293 K) except for the 20 wt % solution measured at 263 K. In order to avoid an overlap of the scattering profiles, the intensity levels for the 30, 25, and 20 wt % solutions were shifted down by one decade relative to those for the 100, 30, and 25 wt % solutions, respectively.

samples were held for about 15 min before measurements with measuring times of about 45 min. The SAXS profiles were desmeared for slit-width and slit-height smearings and corrected for absorption and air scattering as described elsewhere.[24] The absolute SAXS intensity was obtained using the nickel-foil method.[26]

II-C. Dielectric Spectroscopy. Dielectric measurements were carried out with a transformer bridge (General Radio 1615 A) in the frequency range from 100 Hz to 16 kHz. An LCR meter (Hewlett-Packard 42984A) was also used to cover the range from 10 to 100 kHz. Details of the dielectric cell were reported previously.[27] Dielectric measurements were made in the heating direction. First a cryostat[27] containing the cell was immersed in an ethanol bath regulated to the lowest temperature of a series of measurements and allowed to stand for 3 h to ensure temperature equilibrium. After the measurement was made at the lower temperature, the temperature of the bath was raised 2−10 K and again equilibrated for 3 h. The same procedure was repeated up to the highest temperature of the series. Above 310 K, a water bath was used.

III. Experimental Results

III-A. SAXS. The SAXS profiles measured for SI solutions with various polymer concentrations are shown in Figure 1 with a double logarithmic scale. All the profiles are those from the ordered state, as will be clarified later. The quantity q is the magnitude of the scattering vector defined by

$$q = (4\pi/\lambda)\sin(\theta/2) \qquad (1)$$

where λ and θ are the wavelength and scattering angle in the medium, respectively. All the data except that for the 20 wt % solution were obtained at the room temperature. The profile for the 20 wt % solution is that at 263 K because this solution is in the disordered state at room temperature. The profiles for the 20, 25, and 30 wt % solutions were desmeared as described in section II-B. However, the profile for the bulk (100%) was not desmeared for slit-width and slit-height smearings, but the smearing effects are expected to be very small since the experiments were conducted under the condition giving rise to the minimal smearing effects for the highly oriented system, as elucidated earlier.[28] Except for the 20 wt % solution, all the profiles show the high-order scattering maxima at the peak positions of the integer multiples relative to the peak position of the first-order maxima, as shown with numbered arrows, indicating the order. The 20 wt % solution exhibits the first-order maximum and a broad higher order maximum or shoulder. Arrow 2 shows the expected peak position for the second-order maximum from the lamellae for the sake of convenience.

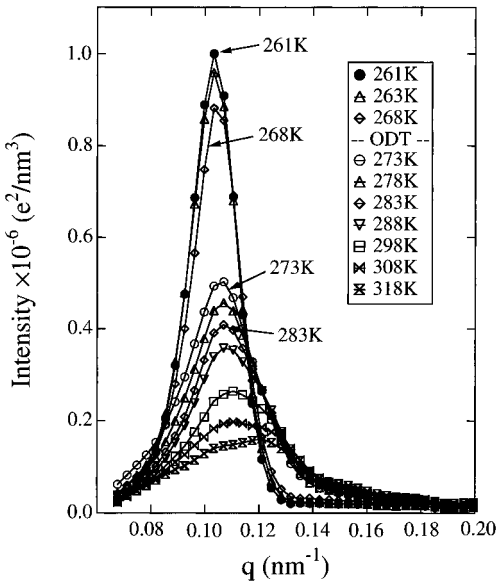

Figure 2. SAXS profiles for the toluene solution containing 20 wt % SI(92−80) at various temperatures.

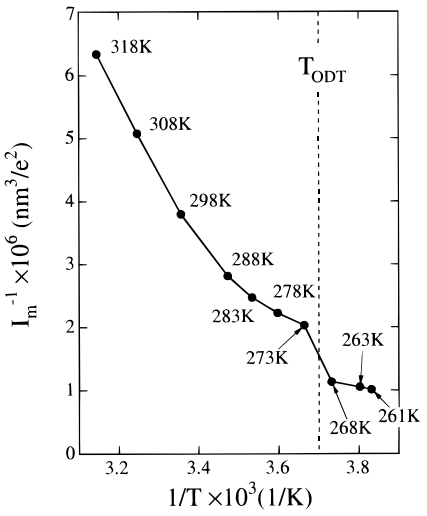

Figure 3. Inverse maximum intensity, I_m^{-1}, plotted as a function of $1/T$ for 20 wt % SI(92−80).

Figure 2 shows the SAXS profiles near the first-order peak, in linear scale, for the 20 wt % SI(92−80) solution measured at various temperatures from 261 to 318 K. The scattered intensity increases and the peak position shifts to a smaller value of q with decreasing temperature. A sharp and remarkable change in the profiles is clearly discerned at temperatures between 268 and 273 K. This discontinuous change of the profiles enables

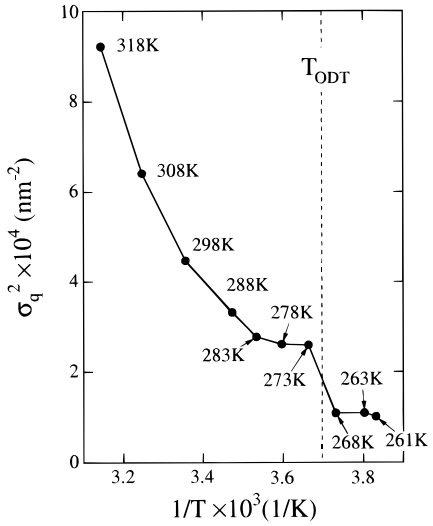

Figure 4. Square of half-width at half-maximum of the first-order SAXS maximum, σ_q^2, plotted as a function of $1/T$ for 20 wt % SI(92−80).

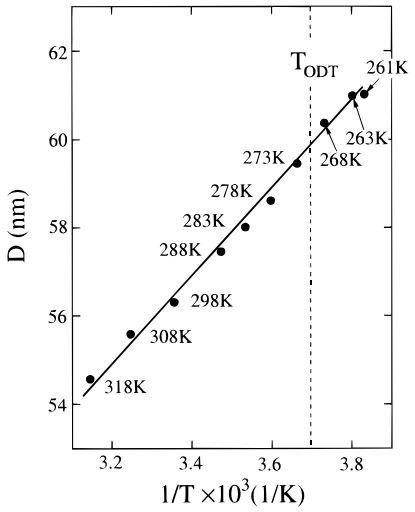

Figure 5. Characteristic length, D, determined from the scattering vector, q_m, at the first-order scattering maximum plotted as a function of $1/T$ for 20 wt % SI(92−80).

us to determine the ODT temperature, T_{ODT}, as 268 K < T_{ODT} < 273 K.

In Figures 3 and 4, the inverse peak scattered intensity, I_m^{-1}, and the squares of half-width at half-maximum, σ_q^2, are plotted as a function of the inverse absolute temperature, $1/T$, respectively. They show that the discontinuous change in I_m^{-1} and σ_q^2 exists between 268 and 273 K, as shown by a vertical broken line. Figure 5 shows the characteristic wavelength, D, plotted as a function of $1/T$. D is defined as

$$D \equiv 2\pi/q_m \qquad (2)$$

where q_m is magnitude of the scattering vector which gives the maximum scattered intensity. The value of D appears to increase linearly from 54 to 61 nm with $1/T$, and no remarkable change is discerned at T_{ODT}.

III-B. Dielectric Relaxation. Figure 6A shows the frequency dependence of the dielectric loss factor, ϵ'', normalized by the weight fraction ϕ_I of the PI block for the 20 wt % solution of SI(92−80) in toluene. As is seen in this figure, the ϵ'' curves below 268 K exhibit two maxima, but above 273 K a single one. The transition temperature is determined to be 271 ± 2 K. This

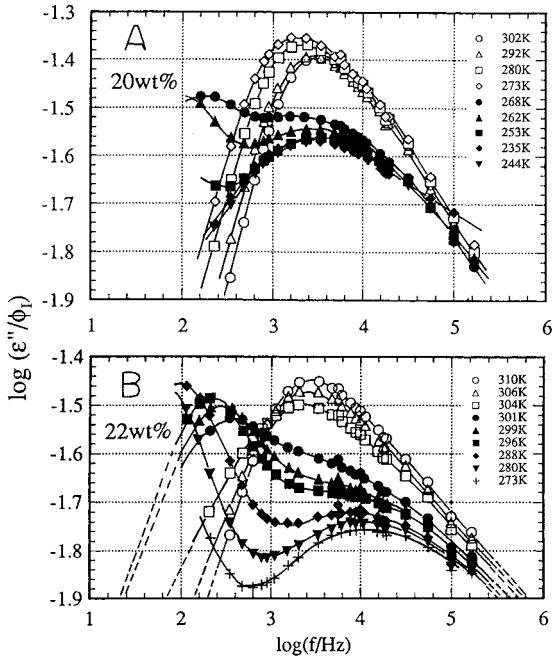

Figure 6. Double logarithmic plot of dielectric loss, ϵ'', divided by weight fraction of PI block against frequency, f, for solutions of SI(92−80): (A) 20 wt % solution, (B) 22 wt % solution.

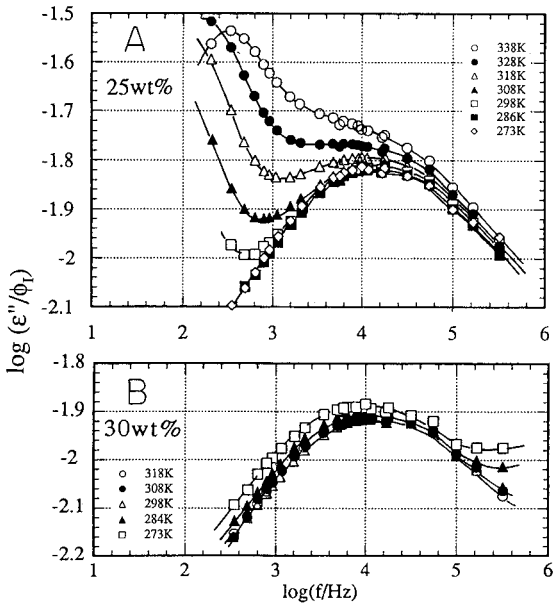

Figure 7. Double logarithmic plot of dielectric loss, ϵ'', divided by weight fraction of PI block against frequency, f, for solutions of SI(92−80): (A) 25 wt % solution, (B) 30 wt % solution.

transition temperature agrees well with T_{ODT} determined by SAXS. Therefore, we conclude that the transition detected by the dielectric spectroscopy corresponds to ODT.

Figures 6B and 7A,B show the ϵ'' curves for the 22, 25, and 30 wt % solutions, respectively. T_{ODT} for the 22 wt % solution is 302 K, as is seen in Figure 6B, indicating that T_{ODT} is very sensitive to concentration. A linear extrapolation of T_{ODT} of the 20 and 22 wt % solutions leads to a T_{ODT} value for the 25 wt % solution of ca. 345 K (see section IV-B later). Therefore, all curves shown in Figure 7 are those in the ordered state. In Figures 6A,B and 7A, the low-frequency peak shifts to a low-frequency side with decreasing temperature, while the high-frequency peak hardly shifts with temperature. The shift of the low-frequency peak with

temperature is particularly obvious for the 22 wt % solution (Figure 6B). Therefore, it is reasonable to consider that the ϵ'' curve for 30% solution is also bimodal: The ϵ'' peak seen in Figure 7B corresponds to the high-frequency peak, and the corresponding low-frequency peak locates in the frequency range far below our experimental window. To summarize, we have observed that the ϵ''/ϕ_I curves of SI(92−80) solutions exhibit a single peak above the ODT and a double peak below the ODT.

IV. Discussion

IV-A. SAXS. Leibler's Landau type mean-field theory[3] predicts that the scattered intensity ($I(q)$) from block copolymer melts in the disordered state is given by

$$[I(q)/N]^{-1} \sim F(q) - 2\chi N \tag{3}$$

$F(q)$ is a function which depends on the radius of gyration (R_g) and composition of the block copolymer under consideration, and χ is the Flory−Huggins' segmental interaction parameter.[3]

The theory for the block copolymer melts has been generalized to semidilute block copolymer solutions[29,30] with renomalization group effects. In the case when the pseudobinary approximation[31] is valid for the solution, we recover a simple scattering formula given by eq 3, where R_g and χ are replaced by the corresponding quantities in semidilute solutions.[32] If χ changes with T according to

$$\chi = A + B/T \tag{4}$$

we can derive the following relation from eqs 3 and 4

$$\begin{aligned}[I(q_m)]^{-1} = {I_m}^{-1} &\sim F(q_m)/N - 2\chi \\ &\sim 2(\chi_s - \chi) \\ &\sim 1/T_s - 1/T \end{aligned} \tag{5}$$

where T_s is the mean-field spinodal temperature and χ_s is the χ-value at T_s. The scattering function $I(q)$ in eq 3 can be rewritten as follows

$$I(q) \sim I_m/[1 + (q - q_m)^2\xi^2] \tag{6}$$

at q close to q_m, where ξ is the thermal correlation length for the concentration fluctuations of PS and PI block chains in the disordered state. σ_q is equal to $1/\xi$ in the disordered state, so the Landau mean-field theory predicts that

$$\begin{aligned}{\sigma_q}^2 = 1/\xi^2 &\sim (1/{R_g}^2)(\chi_s - \chi)/\chi_s \\ &\sim \frac{1}{N}(\chi_s - \chi)/\chi_s \\ &\sim 1/T_s - 1/T \end{aligned} \tag{7}$$

Equations 5 and 7 indicate that both ${I_m}^{-1}$ and ${\sigma_q}^2$ decrease linearly with $1/T$ in the disordered state, in the context of the mean-field theory.

Figure 1 clearly indicates that solutions having SI concentrations higher than 25 wt % have lamellar microdomains with a long-range spatial order. Figure 1 together with Figures 2−4 also shows that the 20 wt % solution at 263 K is in the ordered state. A comparison of the profiles for the 25 and 30 wt % solutions indicates that the relative peak heights of the first- to fourth-order maxima are approximately independent of the polymer concentration, revealing that the relative volume of the PI and PS lamellae is unchanged with polymer concentration. If this is the case down to the 20 wt % solution, the 20 wt % solution also is expected to have the lamellar morphology with the long range order being less than that for the 25 and 30 wt % solutions. In fact, the broad higher order peak or shoulder (marked by arrow 2) may correspond to the second-order peak of the lamellar morphology. Thus we expect that the 22 wt % solution has also the lamellar morphology, though the SAXS experiment was not conducted.

In Figures 3 and 4 both ${I_m}^{-1}$ vs $1/T$ and ${\sigma_q}^2$ vs $1/T$ show a downward convex curvature in the disordered state ($T \geq 273$ K), in contradiction to eqs 5 and 7: ${I_m}^{-1}$ and ${\sigma_q}^2$ deviate upward from the mean-field behavior, such that the values of ${I_m}^{-1}$ and ${\sigma_q}^2$ are larger than those predicted by the mean-field theory. This deviation from the mean-field behavior is interpreted as a consequence of the thermal noise effect[4,5] (the Brazovskii effect[33]). Furthermore, the upward deviation of ${I_m}^{-1}$ and ${\sigma_q}^2$ implies that the random thermal force tends to suppress the concentration fluctuations driven by the net repulsive segmental interaction between different block chains. In other words, the concentration fluctuations and thermal correlation length in real disordered systems are smaller than the values predicted by the mean-field theory.

This effect of the thermal noise on ${I_m}^{-1}$ and ${\sigma_q}^2$ becomes increasingly important when temperature is lowered toward T_s. It was found that even in some temperature range below T_s ($T_{ODT} < T < T_s$), the system still stays in the disordered state (fluctuation-induced disorder). On the other hand, at much higher temperature than T_{ODT}, the effect of the thermal noise becomes small, because the amplitude of the concentration fluctuations is very small and its relaxation time is very short. Consequently, the system can be approximately described by the mean-field theory at such temperatures. Thus we can define the crossover temperature, T_{MF}, from the disordered state characterized by the Brazovskii-type non-mean-field theory to the disordered state characterized by the Leibler-type mean-field theory. T_{MF} was actually observed in some block copolymer melt systems.[6] In this experiment, however, the mean-field behavior (i.e., the linear relationship of ${I_m}^{-1}$ and ${\sigma_q}^2$ with $1/T$) was not clearly observed even at the highest temperature covered. We expect that T_{MF} of this block copolymer solution is higher than 318 K.

Figures 3 and 4 also show that the discontinuous changes in ${I_m}^{-1}$ and ${\sigma_q}^2$ exist at T_{ODT} (268 K < T_{ODT} < 273 K), indicating that the discontinuity observed in bulk block copolymer systems[5−10,34] can be found in the semidilute block copolymer solutions as well. This sharp discontinuity indicates that the ODT is the thermally induced first-order phase transition.[4]

In Figure 5, the value of D appears to change linearly with $1/T$, and no remarkable change is observed at T_{ODT}. This trend is typically observed for the ODT of the block copolymer melts which form lamellar microdomains in the ordered state.[5,6]

IV-B. Dielectric Relaxation. From the SAXS analyses discussed above, we note that all the dielectric relaxation spectra at $T < T_{ODT}$ correspond to those of the lamellar morphology. This is especially obvious for 25 and 30 wt % solutions. Yao et al.[22] interpreted the bimodal dielectric loss peak as follows: The loss peak

at the high frequency side is due to the fluctuation of the junction point of the PS and PI blocks in the direction perpendicular to the interface; on the other hand, the low-frequency peak was assigned to the motion of the free end of the PI chains. However, our recent analyses of the dielectric data on semidilute solutions of polystyrene-*block*-polyisoprene-*block*-polystyrene triblock copolymers indicate that the low-frequency process corresponds to the fluctuation of the S−I junction points and the high frequency loss to the fluctuations of the end-to-end vector of PI block chains.[23] Those analyses as well as discussion of the dynamics of SI will be reported elsewhere. For bulk SI block copolymers with relatively low molecular weight, Fytas and his co-workers reported studies on dielectric relaxation, SAXS, and depolarized light scattering near the ODT.[15,16,35] They observed a bimodal dielectric loss curve and attributed the fast and slow process to the reorientation of the polyisoprene chain and the relaxation of the conformal interface, respectively.

Here we briefly describe the interpretation of our dielectric loss shown in Figure 6 and 7 as follows.

(i) At $T < T_{ODT}$, the frequency dependence of the dielectric loss shows double peaks. The high-frequency loss is associated with the fluctuation of the end-to-end vector of the PI block in the lamellar microdomain and the frequency at the loss peak, f_{max}, is almost independent of temperature, indicating that the dynamics relevant to this loss process are not significantly affected by the segregation power χN. The low-frequency loss is associated with the fluctuation of the SI junctions at the interface of the lamellae, and the f_{max} decreases significantly with lowering temperature. The dynamics is slowed down with increasing segregation power, hence sharpening the interface.

(ii) At $T > T_{ODT}$, the dielectric loss shows a single peak for which f_{max} is close to that for the high-frequency loss peak in the ordered state and f_{max} does not significantly change with temperature. The loss process may be primarily associated with the fluctuation of the end-to-end vector of PI in the disordered state.

From the dielectric relaxation strength, $\Delta\epsilon$, the mean square end-to-end distance, $\langle R_I^2\rangle$, of the PI block can be determined:[23,36]

$$\Delta\epsilon/\phi_I = 4\pi N_A \mu^2 \langle R_I^2\rangle/(3k_B T M_I) \tag{8}$$

where N_A is Avogadro's number, μ the dipole moment per unit contour length, and M_I the molecular weight of the PI block. We determined $\Delta\epsilon$ from the area of the ϵ'' versus log f curve for the 22 wt % SI(92−80) solution by extrapolating the ϵ'' curve as shown by the dashed lines in Figure 6B. The result of the calculation indicates that $\langle R_I^2\rangle^{1/2}$ is 31 nm in the disordered state (310 K) and 33 nm in the ordered state (296 K). Thus the end-to-end distance is close to $D/2$ shown in Figure 5. The expansion factor defined by $\alpha^2 = \langle R_I^2\rangle/\langle R_I^2\rangle_o$ for the PI block is 1.8 and 1.9 in the disordered (310 K) and ordered state (296 K), respectively. Here $\langle R_I^2\rangle_o$ is the mean square end-to-end distance of the homo PI chains in the unperturbed state, and the M_I dependence of α^2 was reported previously.[36] The high expansion factor observed here is partly due to the excluded volume effect in a good solvent (toluene) and partly to the repulsive interaction between the PI and PS block chains.

IV-C. Concentration Dependence of T_{ODT}. In Figure 6, we have seen that T_{ODT} increases from 271 to 302 K as the concentration increases from 20 to 22 wt %. For a qualitative argument of the concentration dependence of T_{ODT}, we assume that the effective χ-value, χ_{eff}, of block copolymer in solution is approximately expressed by[31,32,37]

$$\chi_{eff} = \phi_p \chi \tag{9}$$

where ϕ_p is the polymer volume concentration of the sample and χ is the χ-value of the block copolymer in a melt. The renomalization group analysis[31,32] showed that eq 9 is a good approximation for semidilute Θ solutions with neutral solvents for both block chains. χ is given by $\chi = A_0 + B_0/T$ and usually $A_0 \ll B_0/T$,[38] so we obtain

$$T_{ODT,solution} \cong \phi_p T_{ODT,melt} \tag{10}$$

where $T_{ODT,solution}$ is the T_{ODT} of the block copolymer solution with the concentration ϕ_p and $T_{ODT,melt}$ is that of the block copolymer melt. If T_{ODT} of the 20 wt % block copolymer solution is 271 K, eq 10 predicts that T_{ODT} of the 22 wt % solution is 298 K, which agrees approximately with experimental T_{ODT} for the 22 wt % solution.

Let us further analyze semiquantitatively the concentration dependence of the ODT based upon the assumption that our solutions are semidilute solutions in a commonly good solvent. The relationship among the concentration, ϕ_p, interaction parameter, χ, and degree of polymerization, N, at ODT of semidilute solutions of diblock copolymers in a commonly good solvent was studied theoretically by Fredrickson and Leibler[29] and Olvera de la Cruz:[30]

$$(\phi_p^{1.60}\chi N)_{ODT} = G(f)/2 \tag{11}$$

where $G(f)$ is constant and is a function of the volume fraction f of one of the blocks. When $f = 0.5$, G is close to 21. It follow from this equation that ϕ_p at ODT scales as

$$\phi_{p,ODT} \propto (\chi N)^{-0.62} \tag{12}$$

Recently Lodge et al.[39] tested this equation for semidilute and concentrated solutions of symmetric SIs in toluene and poly(ethylenepropylene)-*block*-poly(ethylethylene) (PEP−PEE) in squalane. They found that eqs 11 and 12 hold well for the SI/toluene system over a wide concentration range. For the PEP−PEE/squalene system, they obtained the exponent −0.81 for eq 12.

On the basis of eqs 11 and 12, we compare the present T_{ODT} data with those reported by Yao et al.[22] for toluene solutions of SI(42−42) in which the molecular weights of PS and PI blocks are 42 000 and 42 000, respectively. The interpolation of the T_{ODT} data indicates that at 300 K, the $\phi_{p,ODT}$ is 0.287 (31 wt %) for SI(42−42) and $\phi_{p,ODT}$ = 0.201 (22 wt %) for SI(92−80). Here we assumed the additivity of the densities to calculate ϕ_p. These values give the exponent of eq 12 as −0.51, which is slightly smaller than the theoretical value. This disagreement may be partly due to the slight difference in the composition of the SIs. Thus the T_{ODT} data obtained here is approximately consistent with that reported by Yao et al.

Lodge et al. determined the parameters of eq 4 for SI solutions: $A = 0.0228$ and $B = 33$. Using these parameters, the values of $\chi N\phi_p^{1.6}$ for SI(42−42) and SI(92−80) were calculated to be 10.0 and 11.4, respec-

tively. Here N was calculated by taking the volume of the styrene monomer as that of the unit. These values are slightly different from the theoretical value 10.5. We note that SI(92−80) solutions used here are in semidilute regime, but those used by Yao et al. were in the regime of concentrated solution. Thus $G(f)$ in eq 11 changes depending on the concentration regime, as indicated theoretically.[30]

V. Conclusion

The order−disorder transition for a semidilute solution of polystyrene-*block*-polyisoprene diblock copolymers were investigated by using SAXS and dielectric relaxation methods. Both methods clearly revealed a sharp ODT, and T_{ODT} determined by SAXS and T_{ODT} by dielectric relaxation agree within experimental error. The SAXS results indicated that I_m^{-1} and σ_q^2 change discontinuously at T_{ODT}, suggesting that the ODT for the semidilute block copolymer solutions studied here is the thermally induced first-order phase transition.

Acknowledgment. This work was supported in part by a Grant-in-Aid for Scientific Research on Priority Areas, "Cooperative Phenomenon in Complex Liquids" (07236103), and by a Grant-in-Aid for Encouragement of Young Scientists A (00086608), both from the Ministry of Education, Science, Sports, and Culture, Japan.

References and Notes

(1) See, for example, a review article: Hashimoto, T. *Thermoplastic Elastomers*, Legge, N. R., Holden, G. R., Schroeder, H. E., Eds.; Carl Hanser Verlag: Vienna, 1987; Chapter 12, §3, (1st ed.) and 2nd ed., in press, and references cited therein.
(2) See, for example, a review article: Bates, F. S.; Fredrickson, G. H. *Annu. Rev. Phys. Chem.* **1990**, *41*, 525 and references cited therein.
(3) Leibler, L. *Macromolecules* **1980**, *13*, 1602.
(4) Fredrickson, G. H.; Helfand, E. *J. Chem. Phys.* **1987**, *87*, 697.
(5) Bates, F. S.; Rosedale, J. H.; Fredrickson, G. H. *J. Chem. Phys.* **1990**, *92*, 6255.
(6) Sakamoto, N.; Hashimoto, T. *Macromolecules* **1995**, *28*, 6825.
(7) Stühn, B.; Mutter, R.; Albrecht, T. *Europhys. Lett.* **1992**, *18*, 427.
(8) Wolff, T.; Burger, C.; Ruland, W. *Macromolecules* **1993**, *26*, 1707.
(9) Hashimoto, T.; Ogawa, T.; Han, C. D. *J. Phys. Soc. Jpn.* **1994**, *63*, 2206.
(10) Floudas, G.; Pakula, T.; Fischer, E. W.; Hadiichristidis, N.; Pispas, S. *Acta Polym.* **1994**, *45*, 176.
(11) Han, C. D.; Kim, J. *J. Polym. Sci. Part B, Polym. Phys.* **1987**, *25*, 1741, Han, C. D.; Kim, J.; Kim, J. K. *Macromolecules* **1989**, *22*, 383.
(12) Pakula, T.; Saijo, K.; Hashimoto, T. *Macromolecules* **1985**, *18*, 2037.
(13) Lin, C. C.; Jonnalagadda, S. V.; Kesani, P. K.; Dai, H. J.; Balsara, N. P. *Macromolecules* **1994**, *27*, 7769.
(14) Amundson, K. R.; Helfand, E.; Patel, S. S.; Quan, Z.; Smith, S. D. *Macromolecules* **1992**, *25*, 1935.
(15) Floudas, G.; Fytas, G.; Hadjichristidis, N.; Pitsikalis, M. *Macromolecules* **1995**, *28*, 2359.
(16) Karatasos, K.; Anastasiadis, S. H.; Floudas, G.; Fytas, G.; Pispas, S.; Hadjichristidis, N.; Pakula, T. *Macromolecules* **1996**, *29*, 1326.
(17) Jian, T.; Anastasiadis, S. H.; Fytas, G.; Adachi, K.; Kotaka, T. *Macromolecules* **1993**, *26*, 4706.
(18) Jian, T.; Anastasiadis, S. H.; Semenov, A. N.; Fytas, G.; Fleischer, G.; Vilesov, A. D. *Macromolecules* **1995**, *28*, 2439.
(19) Boudenne, N.; Anastasiadis, S. H.; Fytas, G.; Xenidou, M.; Hadjichristidis, N.; Semenov, A. N.; Fleischer, G. *Phys. Rev. Lett.* **1996**, *77*, 506.
(20) Pan, C.; Maurer, W.; Lin, Z.; Lodge, T. P.; Stepanek, P.; Von Merwall, E. D.; Watanabe, H. *Macromolecules* **1995**, *28*, 1643.
(21) Balsara, N. P.; Perahia, D.; Safinya, C. R.; Tirrell, M.; Lodge, T. P. *Macromolecules* **1992**, *25*, 3896.
(22) Yao, M. L.; Watanabe, H.; Adachi, K.; Kotaka, T. *Macromolecules* **1992**, *25*, 1699.
(23) Adachi, K.; Kotaka, T. *Prog. Polym. Sci.* **1993**, *18*, 585.
(24) Hashimoto, T.; Suehiro, S.; Shibayama, M.; Saijo, K.; Kawai, H. *Polym. J.* **1981**, *13*, 501. Fujimura, M.; Hashimoto, T.; Kawai, H. *Mem. Fac. Eng., Kyoto Univ.* **1981**, *43 (2)*, 224, Suehiro, S.; Saijo, K.; Ohta, Y.; Hashimoto, T.; Kawai, H. *Anal. Chim. Acta* **1986**, *189*, 41.
(25) Fujimura, M.; Hashimoto, H.; Kurahashi, K.; Hashimoto, T.; Kawai, H. *Macromolecules* **1981**, *14*, 1196.
(26) Hendricks, R. W. *J. Appl. Crystallogr.* **1972**, *5*, 315.
(27) Imanishi, Y.; Adachi, K.; Kotaka, T. *J. Chem. Phys.* **1988**, *89*, 7585.
(28) Hashimoto, T.; Todo, A.; Itoi, H.; Kawai, H. *Macromolecules* **1977**, *10*, 377.
(29) Fredrickson, G. H.; Leibler, L. *Macromolecules* **1989**, *22*, 1238.
(30) Olvera de la Cruz, M. *J. Chem. Phys.* **1989**, *90*, 1995.
(31) Onuki, A.; Hashimoto, T. *Macromolecules* **1989**, *22*, 879.
(32) Hashimoto, T.; Mori, K. *Macromolecules* **1990**, *23*, 5347.
(33) Brazovskii, A. *Sov. Phys. JETP* **1975**, *41*, 85.
(34) Ogawa, T.; Sakamoto, N.; Hashimoto, T.; Han, C. D.; Baek, D. M. *Macromolecules* **1996**, *29*, 2113.
(35) Karatasos, K.; Anastasiadis, Semenov, A. N.; G.; Fytas, G.; Pitsikalis, M.; Hadjichristidis, N. *Macromolecules* **1994**, *27*, 3543.
(36) Adachi, K.; Nishi, I.; Itoh, S.; Kotaka, T. *Macromolecules* **1990**, *23*, 2550.
(37) Helfand, E.; Tagami, Y. *J. Chem. Phys.* **1972**, *57*, 1812.
(38) Mori, K.; Hashimoto, T. *J. Chem. Phys.* **1996**, *104*, 7765.
(39) Lodge, T. P.; Pan, C.; Jin, X.; Zhao, J.; Maurer, W. W.; Bates, F. S. *J. Polym. Sci. Polym. Phys. Ed.* **1995**, *33*, 2289.

MA9609487